JOURNAL OF GEOPHYSICAL RESEARCH, VOL. 102, NO. D8, PAGES 9387-9395, APRIL 27, 1997

Effect of cloud inhomogeneities on the solar zenith angle dependence of nadir reflectance

Norman G. Loeb[1] and Tamás Várnai
Department of Atmospheric and Oceanic Sciences, McGill University, Montreal, Quebec, Canada

Roger Davies
Institute of Atmospheric Physics, University of Arizona, Tucson

Abstract. A significant discrepancy has been noted between satellite measurements of shortwave reflectance at nadir and the results of plane-parallel model calculations: For moderate to large solar zenith angles, observed nadir reflectances increase with solar zenith angle, whereas plane-parallel values decrease. Consequently, cloud optical depths retrieved using one-dimensional (1-D) theory have a bias which increases systematically with solar zenith angle. Using Monte Carlo model simulations of photon transport through stochastic, isotropic, scale-invariant cloud fields with variable cloud top heights and volume extinction coefficients, we show that nadir reflectances from three-dimensional cloud fields increase with solar zenith angle, consistent with the observations. The difference from the 1-D case is shown to be explainable by cloudside illumination as well as by the presence of structured (i.e., non-flat) cloud tops. Cloud sides enhance the amount of incident solar radiation intercepted by cloud, allowing more radiation to be scattered upward in the nadir direction. Structured cloud tops change the slope of illuminated cloud top surfaces, such that nadir reflectance at low solar elevations increases with the slope of the illuminated surface. For simple cloud geometries the two effects make equivalent contributions to the increase in nadir reflectance with solar zenith angle. While this increase is most pronounced for vertically extensive broken cloud fields, it also affects reflectances from overcast cloud fields with inhomogeneous (bumpy) cloud tops. Thus the observed solar zenith angle bias in cloud optical depth for the general cloud scene likely also occurs for extensive overcast cloud fields. Internal inhomogeneities due to small-scale liquid water content variations within clouds are shown to cause no changes at low Sun and only slight decreases in nadir reflectance for high solar elevations.

1. Introduction

In a recent study, *Loeb and Davies* [1996] showed that use of the one-dimensional (1-D) approach to infer cloud optical depth directly from observations at near-nadir views can lead to substantial solar zenith angle dependent biases in cloud optical depth, especially for thicker clouds. When plane-parallel model calculations were matched to 1 year of Earth Radiation Budget satellite shortwave observations over ocean between 30°N and 30°S on a pixel-by-pixel basis by adjusting cloud fraction and cloud optical depth, the resulting frequency distributions of cloud optical depth showed a systematic shift toward larger values with increasing solar zenith angle. The reason was shown to be due to a fundamental difference between the observed and plane-parallel model reflectance dependence on solar zenith angle: on average, observed nadir reflectances increase with solar zenith angle, whereas 1-D nadir reflectances show the opposite behavior.

The aim of the present study is to provide a physical explanation for the observational results of *Loeb and Davies* [1996]. In that study it was suggested that three-dimensional (3-D) cloud effects may be responsible for the observed discrepancy, and preliminary Monte Carlo simulations involving 3-D cloud fields appeared to support this hypothesis. Here we extend that analysis and examine the relative importance of (1) cloud external inhomogeneities, that is, cloud sides and cloud top structure and (2) cloud internal inhomogeneities associated with liquid water content variations within cloud

[1]Now at College of Oceanic and Atmospheric Sciences, Oregon State University, Corvallis.

Paper number 96JD03719.
0148-0227/97/96JD-03719$09.00

elements. To demonstrate the importance of these effects, nadir reflectances from 3-D and 1-D cloud fields are compared as a function of solar zenith angle in a manner analogous to the comparisons between observations and plane-parallel calculations by *Loeb and Davies* [1996]. We investigate the conditions under which the two sets of comparisons yield similar qualitative results and determine which of the 3-D effects are most responsible for the deviation from 1-D behavior.

The following section briefly describes the Monte Carlo method and the cloud fields considered in the simulations. Comparisons are then made between 3-D and 1-D reflectance calculations, considering external cloud inhomogeneities first and internal inhomogeneities second. Similarities and differences between the 3-D and 1-D model comparisons and the results of *Loeb and Davies* [1996] are highlighted throughout.

2. Monte Carlo Method

The Monte Carlo method of solving radiative transfer problems has been widely used in the past to examine the radiative properties of 3-D cloud fields [*Busygin et al.*, 1973; *McKee and Cox*, 1974; *Wendling*, 1977; *Davies*, 1978; *Welch and Wielicki*, 1984; *Kobayashi*, 1988; *Barker and Davies*, 1992]. The method involves a numerical simulation of the probability laws governing the distance to collision and change of direction as simulated photons move through a scattering medium. Photons are traced through the medium until they escape, taking optical depth, phase function, and single scattering albedo into account.

In this study the Monte Carlo code described by *Várnai* [1996] is used. Simulations are made for a wavelength of 0.865 μm using a Mie phase function for the Sc_{top} cloud model of *Welch et al.* [1980]. While the model can handle atmospheric effects and surface reflection, these are not included here in order to concentrate specifically on clouds. This should not have much influence since atmospheric effects and surface contributions over ocean tend to be small at 0.865 μm. The model divides the cloud field into boxes/grid points, each having a resolution r. It assumes periodic boundary conditions, so that photons leaving one side of a cloud field boundary come back at the opposite side. In all simulations, the number of photons used is 10^6, which gives a reflectance uncertainty of less than 1% [*Várnai*, 1996].

Reflectance is defined as

$$R = \frac{\pi I}{\mu_o F} \times 100\%, \qquad (1)$$

where I is the nadir radiance, F is the incident solar flux, and μ_o is the cosine of the solar zenith angle.

The advantage of the Monte Carlo approach is that it can determine radiative properties for any cloud geometry. Here simulations are performed using stochastic, isotropic, scale-invariant cloud fields [*Barker and Davies*, 1992] characterized by continuous power spectra. As a first approximation, their structure is represented by the cloud fraction and slope of the wavenumber spectrum of cloud optical depth. For cloud fields which have isotropic spectral densities, the ensemble-averaged one-dimensional spectra $\langle S_k \rangle$ scale according to k^{-s}, where k is the wavenumber and s is the cloud field scaling exponent. The greatest departure from plane-parallel clouds occurs for $s = 0$ (white noise). As s increases, the number of small clouds decreases, and the variability across individual clouds decreases (i.e., clouds become more plane-parallel). In the present study, stochastic cloud fields are generated for various cloud fractions (f) and domain optical depths (τ_d) using the following scaling: $\langle S_k \rangle \sim k^{-1}$ for $k \leq 6$, and $\langle S_k \rangle \sim k^{-3.6}$ for $k > 6$. Cloud fields are defined over a 512 $\times$ 512 grid with a grid point resolution r = 68.7 m. In order to examine the effect of internal inhomogeneities on reflectance, simulations are performed using clouds which have a constant volume extinction coefficient (β_e) of 30 km^{-1} (section 3.1), as well as the case where β_e is allowed to vary within individual cloud elements (section 3.2). As an example, Figure 1 shows a cloud field with $f = 0.5$ and $\tau_d = 5$. This scene has characteristics which appear to resemble a real cloud scene but clearly does not represent the entire range of cloud variability that can be encountered over the

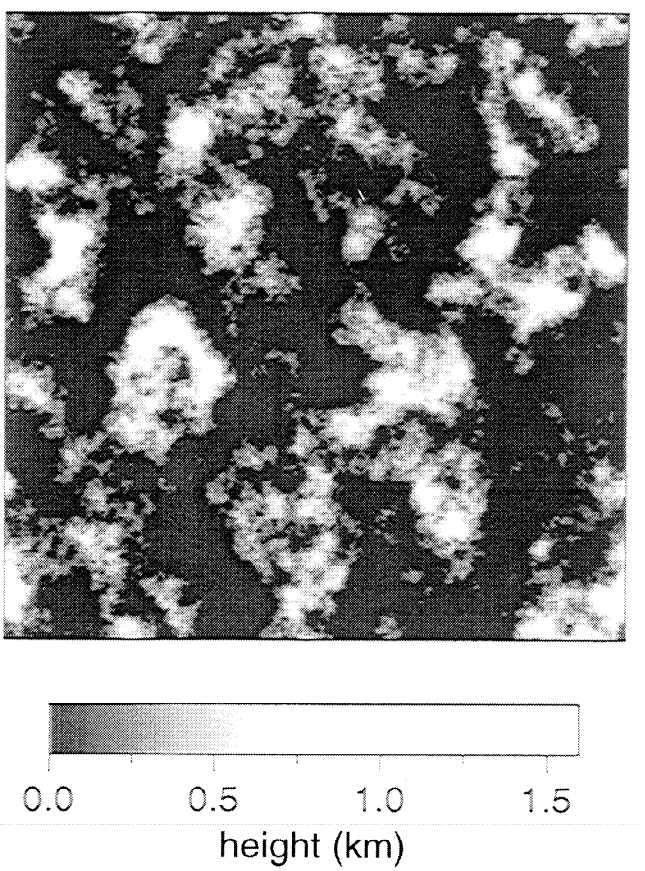

Figure 1. Stochastic cloud field generated under the scaling $\langle S_k \rangle \sim k^{-1}$ for $k \leq 6$, and $\langle S_k \rangle \sim k^{-3.6}$ for $k > 6$, for a cloud fraction $f = 0.5$ and a domain optical depth $\tau_d = 5$.

course of 1 year (as was considered by *Loeb and Davies* [1996]). It serves merely to illustrate the kinds of differences that might be expected between 3-D and 1-D cloud reflectances. In order to investigate the role of cloud top structure, Monte Carlo simulations are also performed using simple cloud shapes consisting of isolated cones of various aspect ratios (defined as the ratio of the vertical dimension to the horizontal dimension).

3. Results

3.1. External Inhomogeneities

As an illustration of how 3-D effects can influence the nadir reflectance dependence on μ_o, Figure 2 shows a comparison between ("scene") reflectances generated using the 3-D cloud field (R_{3D}) in Figure 1 with plane-parallel model calculations (0.5 R_P ($\tau_p = 7.1$)). A constant volume extinction coefficient of 30 km^{-1} is assumed throughout the cloud field. The plane-parallel calculations were normalized at $\mu_o = 0.95$ by adjusting the cloud optical depth to fit the 3-D result, taking cloud fraction into account. This approach is analogous to that used by *Loeb and Davies* [1996] to fit the plane-parallel calculations to the observations. A cloud optical depth of $\tau_p = 7.1$ was found to provide the best match in this case. As shown, 3-D reflectances increase with decreasing μ_o, while the opposite occurs for the 1-D result for $\mu_o < 0.6$. This is qualitatively consistent with the observational results of *Loeb and Davies* [1996] and highlights the importance of including 3-D cloud effects.

To examine how these results depend on cloud fraction (f), Figure 3 compares 3-D reflectances for $f = 0.25$, 0.50, 0.75, and 1.0 at $\tau_d = 5$, with a plane-parallel

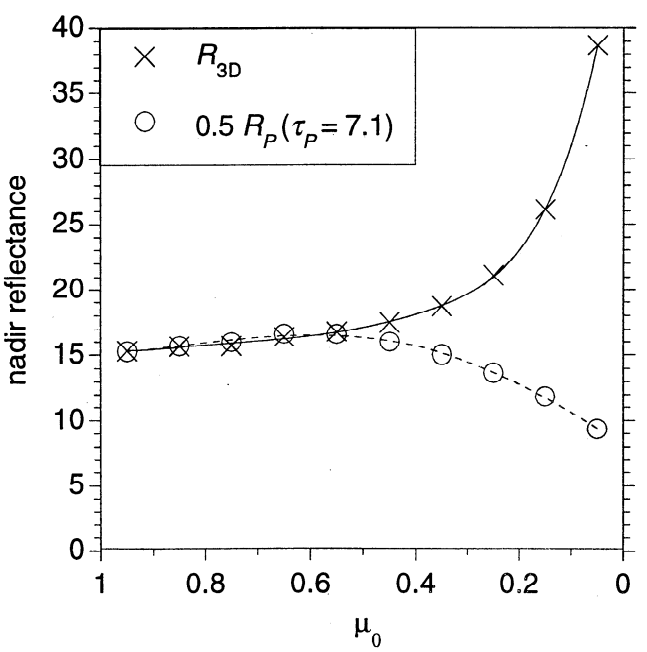

Figure 2. Nadir reflectance as a function of μ_o for the cloud field in Figure 1 (R_{3D}) and a plane-parallel calculation normalized to R_{3D} at $\mu_o = 0.95$.

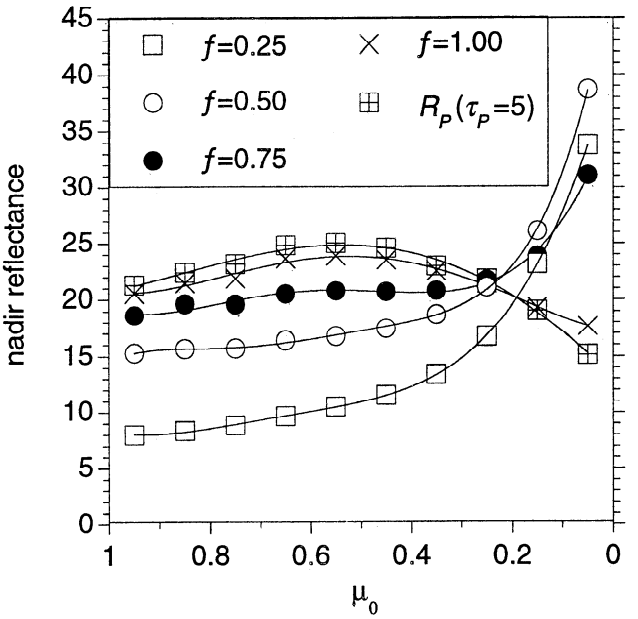

Figure 3. Three-dimensional nadir reflectances as a function of μ_o for various cloud fractions (f) together with a plane-parallel calculation at an optical depth $\tau_p = 5$.

calculation at the same optical depth. Since τ_d is kept constant, the average cloud optical depth of individual 3-D cloud elements within the scene ($< \tau_{3D} >$) is inversely proportional to f (e.g., $< \tau_{3D} > = 20$ for $f = 0.25$; $< \tau_{3D} > = 10$ for $f = 0.5$; etc.). As f increases, the clouds become more homogeneous and optically thinner, and the average cloud aspect ratio decreases. For large μ_o, 1-D reflectances are larger than 3-D values because of diffusive leakage through the sides of the 3-D clouds. This is a classic result which has appeared in many other studies involving Monte Carlo simulations [e.g., *McKee and Cox*, 1974; *Wendling*, 1977; *Davies*, 1978; *Kobayashi*, 1993]. It also explains why a plane-parallel cloud optical depth of only 7.1 rather than 10 provides a match between 3-D and 1-D reflectances at $\mu_o = 0.95$ in Figure 2. As μ_o decreases, 3-D cloud reflectances increase rather substantially for $f < 1$, while the case with $f = 1$ decreases in a manner which is similar to the 1-D result. This apparent agreement with 1-D theory occurs because the cloud top is fairly uniform for this case, not because the cloud field is overcast. Reflectances for an overcast cloud field with larger horizontal variability in its cloud top structure (i.e., a bumpier cloud) can also deviate quite strongly from 1-D results.

To illustrate, Figure 4 shows reflectances generated from overcast cloud fields constructed by inserting a flat cloud layer of optical depth $\tau_b = 5$ beneath the $f = 0.50$ and $f = 0.75$ cloud fields used in Figure 3. These results are labeled $< f_{3D} > = 0.50$, $< \tau_{3D} > = 15$, and $< f_{3D} > = 0.75$, $< \tau_{3D} > = 11.6$, respectively, where $< f_{3D} >$ is the fraction of the domain containing bumpy cloud of average optical depth $< \tau_{3D} >$. Also plotted

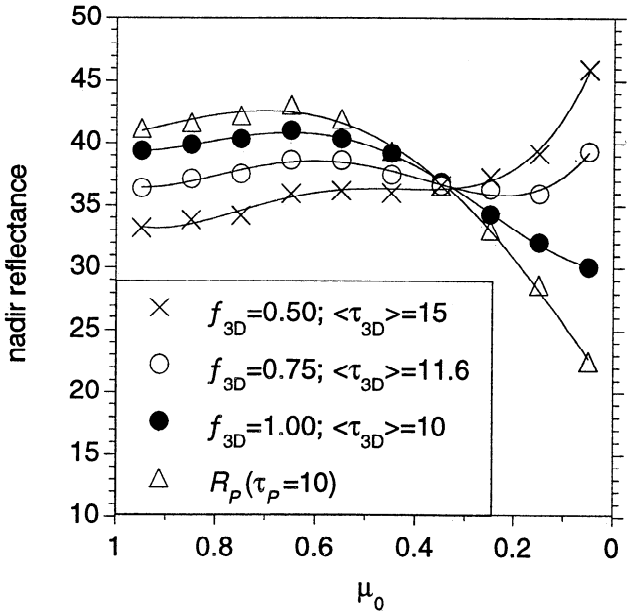

Figure 4. Reflectances generated from overcast cloud fields constructed by inserting a flat cloud base of optical depth $\tau_b = 5$ beneath the $f = 0.50$ and $f = 0.75$ cloud fields in Figure 3. Variable $< f_{3D} >$ is the fraction of the domain containing bumpy cloud of average optical depth $< \tau_{3D} >$. Also plotted is a plane-parallel calculation at an optical depth of 10 ($R_P(\tau_p = 10)$).

is a case with $< f_{3D} > = 1.0$, $< \tau_{3D} > = 10$, and the plane-parallel calculation at an optical depth of 10 ($R_P(\tau_p = 10)$). For the $< f_{3D} > = 0.50$, $< \tau_{3D} > = 15$ case (the bumpiest cloud field), a systematic increase in reflectance with decreasing μ_o is obtained, while for the $< f_{3D} > = 0.75$, $< \tau_{3D} > = 11.6$ case, the increase is less severe and occurs only at very low Sun. Thus, provided the cloud tops are sufficiently inhomogeneous, significant differences between 3-D and 1-D results can occur even for overcast clouds. This result is somewhat surprising since many previous studies have shown that differences between 3-D and 1-D cloud fluxes tend to decrease substantially as cloud fraction approaches unity [*Welch and Wielicki*, 1984]. For remote sensing applications, which often rely on nadir measurements to infer cloud properties, this has important ramifications since it implies that the 1-D cloud optical depth bias with solar zenith angle observed by *Loeb and Davies* [1996] for the general cloud scene may also affect retrievals from extensive overcast cloud fields.

3.1.1. Cloud side illumination. It has long been recognized that one of the main reasons for differences between 3-D and 1-D cloud radiative properties at low Sun elevations is side illumination [*McKee and Cox*, 1974; *Davies*, 1978]. As the Sun becomes more oblique, a greater fraction of the incident solar radiation is intercepted by the sides of 3-D clouds, resulting in more upward scattering than from a cloud of infinite extent. The degree to which side illumination occurs for an individual cloud depends on its shape and aspect ratio. For a cloud field the illumination enhancement also depends on the cloud fraction and the distribution of the cloud elements within the scene [*Welch and Wielicki*, 1984; *Kobayashi*, 1988]. Past studies have focused on simple parameterizations of reflected flux in terms of an "effective cloud fraction," defined as the equivalent cloud fraction of a planiform field of clouds with the same vertical optical depth required to give the same flux as that from a finite cloud field [*Weinman and Harshvardhan*, 1982; *Harshvardhan and Thomas*, 1984; *Welch and Wielicki*, 1984; *Kobayashi*, 1988]. However, these parameterizations are highly idealized due to the simple cloud geometries employed and do not directly apply to remote sensing problems since they consider overall flux rather than radiances/reflectances in a particular direction.

To examine the influence of side illumination on nadir reflectance at different μ_o, cloud fractions for stochastic cloud fields were derived with respect to the solar direction in separate, slightly modified Monte Carlo simulations [*Várnai*, 1996]. In these simulations, once a photon hits a cloud, it is not allowed to continue its path. The number of photons intercepted by cloud divided by the number of incident photons gives the cloud fraction, $f^*(\mu_o)$, illuminated from the solar direction. This definition of cloud fraction is equivalent to that obtained by the product of cloud fraction at $\mu_o = 1$ and the area enhancement ratio, defined as the ratio of the cloud area at μ_o projected onto a horizontal surface to the cloud area at $\mu_o = 1$ [*Welch and Wielicki*, 1984]. Figure 5 shows $f^*(\mu_o)$ as a function of μ_o for the cloud field in Figure 1 ($f = 0.5$), as well as for $f = 0.25$ and $f = 0.75$. Comparing these with the nadir reflectances in Figure 3, there does indeed appear to be a strong link between the corresponding curves: the $f^*(\mu_o)$ curves

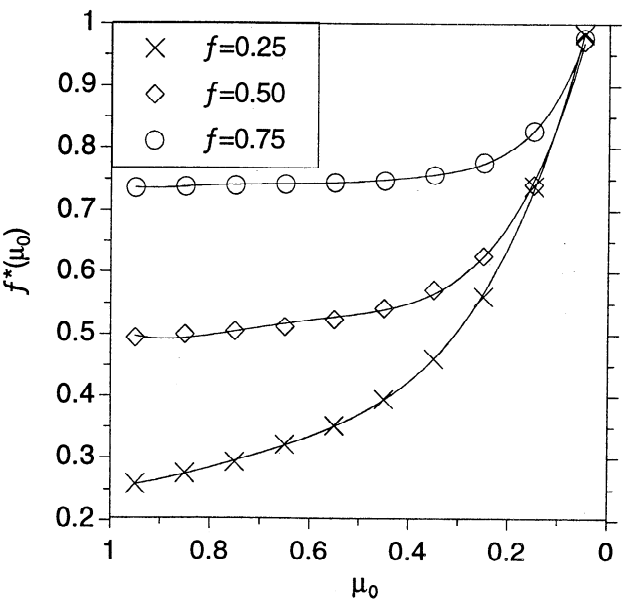

Figure 5. Cloud fraction as viewed from the solar direction, $f^*(\mu_o)$, for cloud fields with nadir cloud fraction $f = 0.25$, $f = 0.50$, and $f = 0.75$.

show a dependence on μ_o which is quite similar to that of nadir reflectance.

If enhanced cloud illumination is the only factor responsible for the increase in nadir reflectance with decreasing μ_o, we might expect agreement between 3-D and plane-parallel results when the enhancement effect is included in the plane-parallel calculations. As a test, the plane-parallel calculations were modified by scaling the reflectance at a given τ_p by $f^*(\mu_o)$ instead of f. Figure 6 shows reflectances for the 3-D cloud field of Figure 1, together with a plane-parallel calculation which assumes $f = 0.5$ at all μ_o, and a case which uses $f^*(\mu_o)$. While this new approach increases reflectances at small μ_o, they are still lower than those for the 3-D case by as much as a factor of 2. Similar results were obtained in comparisons at $f = 0.25$ and $f = 0.75$ (not shown). Thus, while side illumination explains part of the discrepancy between 3-D and 1-D reflectances at small μ_o, it does not account for all of it.

3.1.2. Cloud top structure. The above results are not unexpected since, as was shown in Figure 4, significant differences between 1-D and 3-D reflectances can occur even for overcast clouds, where no enhancement in cloud fraction occurs ($f^*(\mu_o) = 1$ at all μ_o). Instead, differences in Figure 4 appeared to be most sensitive to the cloud top structure. From a modeling viewpoint, cloud top structure is an extremely difficult feature to describe since it is highly variable from cloud to cloud (and even within one cloud for that matter). Further, it is not clear what properties of cloud top structure are important.

One property which may prove to be important is the slope of illuminated cloud top surfaces. Since the angle of incidence of incoming solar radiation relative to a sloped surface is different from that for a flat surface, this can substantially alter the radiation reflected upward. However, since real clouds are highly irregular in shape, many different cloud slopes are presented to the solar beam, making it difficult to study this effect directly.

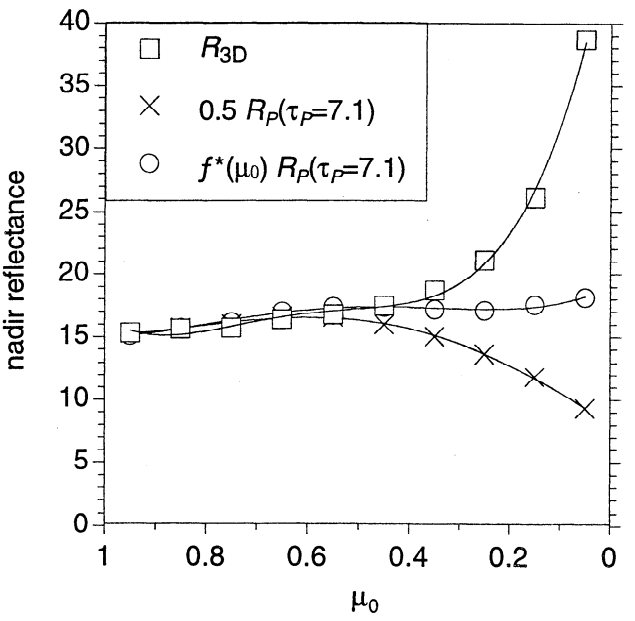

Figure 6. Comparison between the same curves plotted in Figure 2 with a plane-parallel result which accounts for the change in cloud fraction with $\mu_o(f^*(\mu_o)R_P(\tau_p = 7.1))$.

To simplify the problem, it is useful to consider simple cloud geometries. Here separate simulations for cloud fields consisting of isolated cones are performed. The cloud fields are defined so as to ensure a constant cloud fraction of $f = 0.21$ and an average cloud optical depth of $< \tau_c > = 10$, so that the domain optical depth is held fixed at $\tau_d = 2.1$. By varying the horizontal domain size (by modifying the grid point resolution r), while keeping the vertical size and cloud fraction constant, simulations are performed for different aspect ratios α. For a cone, α is related to the slope (γ) of the surface through $\gamma = tan^{-1}(2\alpha)$, so that increasing α increases the slope γ.

To separate the influence of the slope of a surface on nadir reflectance from the enhancement associated with side illumination, we consider how the ratio $R_{3D}/(f^*(\mu_o)R_P)$ changes with α and compare this with results for $R_{3D}/(fR_P)$. In the first ratio, side illumination is accounted for explicitly, while the latter accounts for neither effect. Figure 7a shows $R_{3D}/(f^*(\mu_o)R_P)$ as a function of μ_o for cones with $\alpha = 0.05$, 0.1, 0.2, and 0.5, while Figure 7b shows the same but for $R_{3D}/(fR_P)$. Here ratios are normalized to unity at $\mu_o = 0.95$. When side illumination is accounted for (Figure 7a), the increase in the ratio becomes more pronounced with decreasing μ_o as the slope of the surface gets larger (or as α increases). In fact, the larger the slope of the surface, the sooner this increase occurs. For example, for $\alpha = 0.05$, the ratio increases only when $\mu_o < 0.25$, whereas for $\alpha = 0.5$, it increases when $\mu_o < 0.55$. When both side illumination and slope are involved (Figure 7b), ratios are enhanced by an additional factor of ≈ 2 for $\alpha \geq 0.2$, and much less at smaller α. Thus for highly sloped surfaces the two effects contribute roughly equally to the increase in nadir reflectance with decreasing μ_o.

While a rigorous correction for the slope effect in realistic cloud fields is beyond the scope of this study, an experiment was nonetheless performed to explore one possible approach for the simple cloud geometries as a starting point. Consider a sloped surface inclined at an angle γ relative to the horizontal plane, with solar illumination at $\theta_o(= \cos^{-1}\mu_o)$ and an observer at nadir, as illustrated in Figure 8. Relative to the sloped surface facing the Sun, the angle of incidence becomes $\theta'_o = \theta_o - \gamma$, while the observer view angle is $\theta' = \gamma$, and the relative azimuth about the normal to the surface (z') is given by the angle ϕ'. If we now assume that a surface such as a cone can be approximated by a plane inclined at an angle equal to the slope of the cone, the plane-parallel model can then be used to generate reflectances

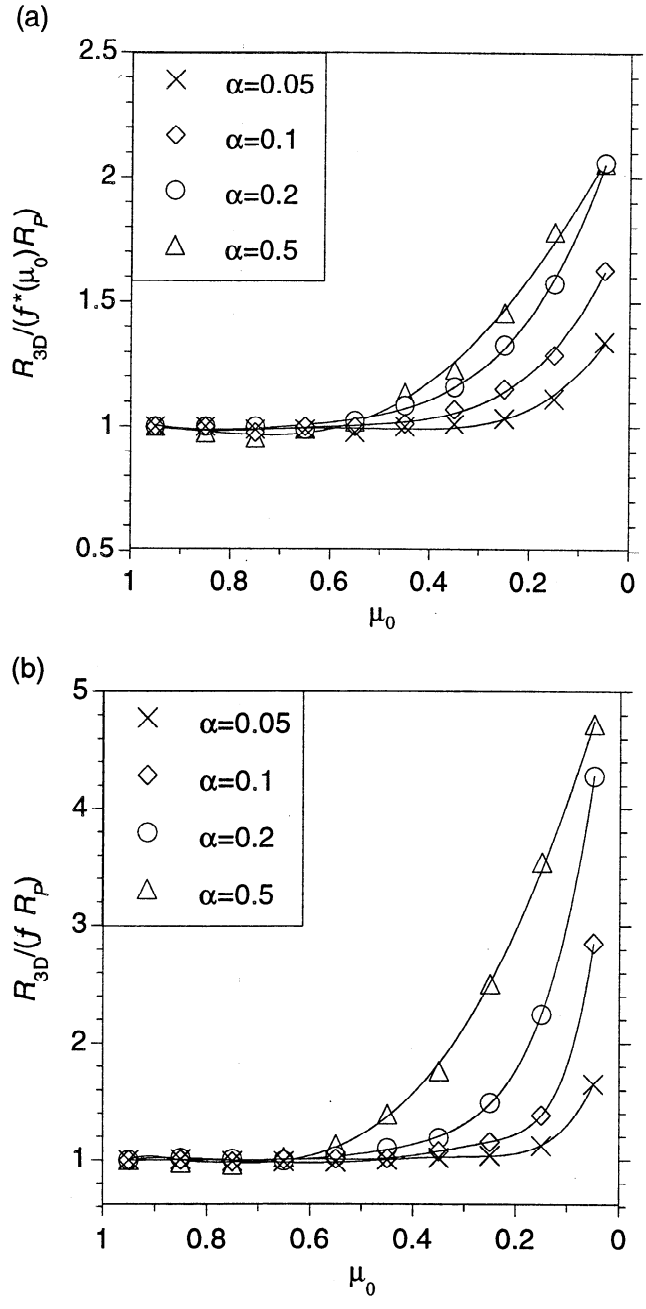

Figure 7. (a) $R_{3D}/(f^*(\mu_o)R_P)$ and (b) $R_{3D}/(fR_P)$ versus μ_o for isolated cones with $\alpha = 0.05$, 0.1, 0.2, and 0.5.

at θ_o', θ', and ϕ', and if the enhancement due to side illumination of the cone is taken into account, these can be compared with the cone reflectances. As a further simplification, since a cone is azimuthally symmetric and its slope does not vary over its surface, reflectances from the plane surface can be averaged over ϕ' in the forward scattering direction ($0° \leq \phi' \leq 90°$; $270° \leq \phi' \leq 360°$) for $\theta_o - \gamma > 0°$, and over the backscattering direction ($90° \leq \phi' \leq 180°$) for $\theta_o - \gamma < 0°$.

Figures 9a-d compare reflectances from an isolated cone (R_{3D}) at $\alpha = 0.05$ ($\gamma = 5.7°$), $\alpha = 0.1$ ($\gamma = 11.3°$), $\alpha = 0.2$ ($\gamma = 21.8°$), and $\alpha = 0.5$ ($\gamma = 45°$), respectively, with plane-parallel calculations (at $\tau_p = 10$) which do not account for the slope effect (0.21 R_P and $f^*(\mu_o)R_P$), and an approximation that takes both slope and enhancement due to cloud side illumination into account ($f^*(\mu_o)R_P'$). While the sloped plane approximation is not perfect, it appears to at least capture the main dependence of 3-D reflectance on solar zenith angle. For example, as α gets larger, both R_{3D} and $f^*(\mu_o)R_P'$ show a progressively stronger increase with decreasing μ_o. For $\alpha < 0.5$ (Figures 9a through 9c), the largest discrepancies now appear at large μ_o, and differences decrease as the Sun tends toward the horizon. This is a substantial improvement over the $f^*(\mu_o)R_P$ case which does not account for the slope effect. Large differences at Sun angles close to zenith are expected since diffusive leakage through the cloud sides is not accounted for. At $\alpha = 0.5$, differences between 3-D cloud reflectances and those for the $f^*(\mu_o)R_P'$ case at small μ_o are likely caused by diffusive leakage through the antisolar side of the 3-D clouds due to a shorter horizontal path length through these clouds. If this did not occur, R_{3D} would likely increase with decreasing μ_o in a manner similar to that for the $f^*(\mu_o)R_P'$ case.

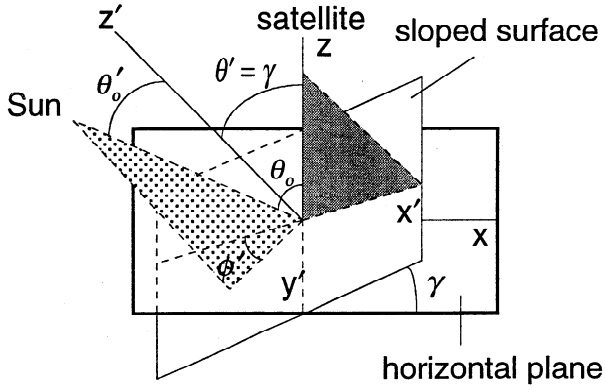

Figure 8. Schematic illustrating incident and observer angles relative to a sloped surface inclined at an angle γ relative to the horizontal plane.

While this approach works reasonably well for simple cloud geometries, clearly a much more rigorous analysis is required to establish its validity for real cloud fields. In that case the slope and orientation of the cloud top surfaces would be required. Also, the effect of side illumination would have to be included, as would the influence of side leakage through the cloud sides (especially at large μ_o). While this would be difficult to do using actual satellite observations, it may be feasible through parameterizations based on Monte Carlo simulations of stochastic 3-D cloud fields.

3.2. Internal Inhomogeneities: Volume Extinction Coefficient Variations

In the previous section it was assumed that the volume extinction coefficient (β_e) is constant throughout the cloud field. However, ground, aircraft, and

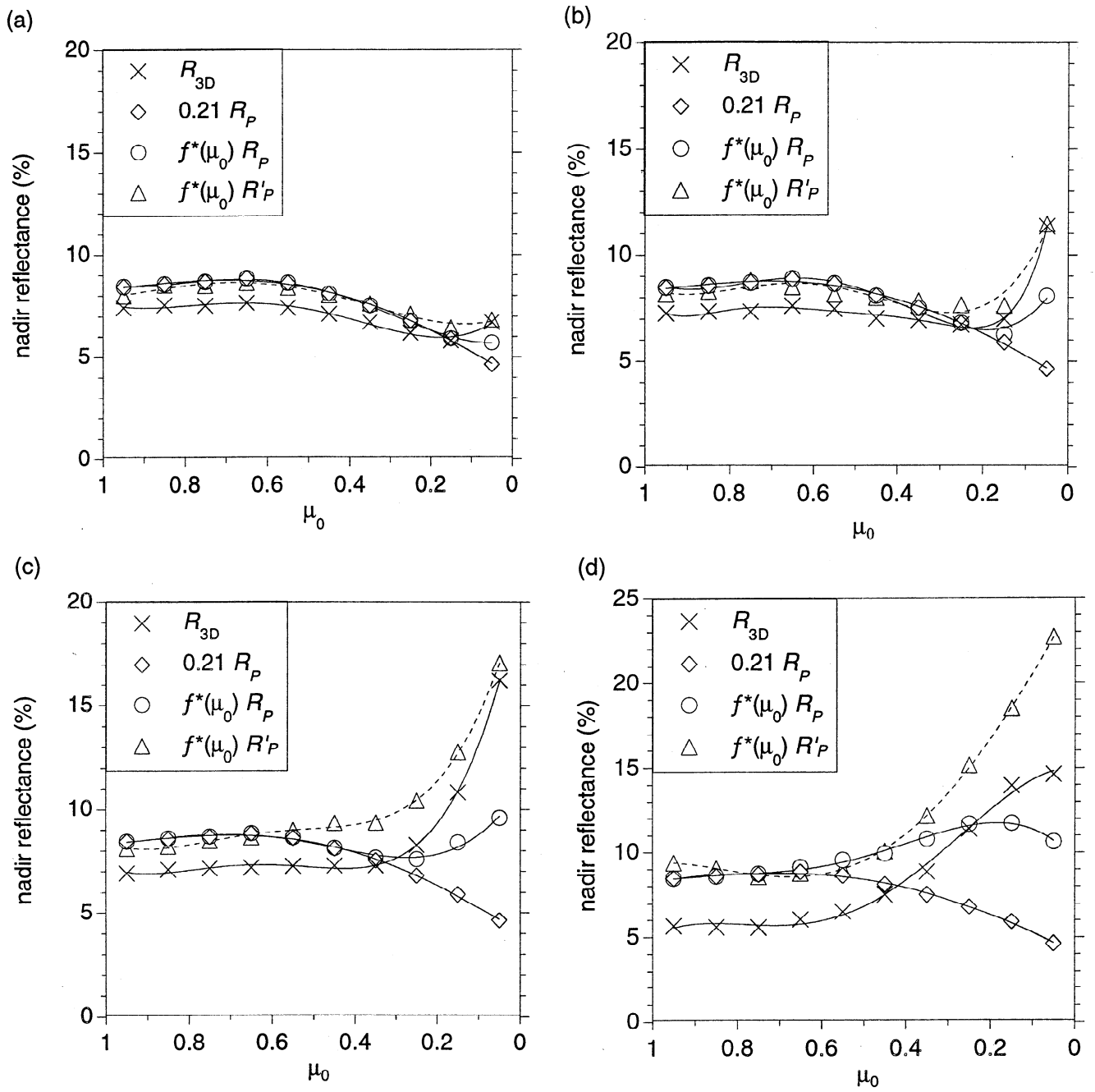

Figure 9. Isolated cone reflectances (R_{3D}) together with various plane-parallel calculations for (a) $\alpha = 0.05$ ($\gamma = 5.7°$), (b) $\alpha = 0.1$ ($\gamma = 11.3°$), (c) $\alpha = 0.2$ ($\gamma = 21.8°$), and (d) $\alpha = 0.5$ ($\gamma = 45°$). R'_p is obtained using incident and observer angles relative to the sloped surface.

satellite measurements [e.g., *Ackerman*, 1967; *Cahalan and Snider*, 1989; *Wielicki and Welch*, 1986] have shown that real clouds exhibit marked internal inhomogeneities associated with spatial variations in liquid water content (and therefore β_e). Previous studies have shown that these variations can cause a "channeling" effect [*Cannon*, 1970; *Cahalan*, 1989; *Davis et al.*, 1990], whereby downwelling radiation from denser portions of the cloud may get preferentially "channeled" into less dense regions, thus reducing cloud albedo relative to internally homogeneous clouds. To test whether or not these variations affect the μ_o dependence of cloud reflectance, simulations were performed using a cloud field which not only possesses cloud top height variations (as in the previous section), but which also possesses 3-D spatial variations in β_e within the cloud elements. The distribution of β_e is obtained by extending the stochastic, scaling variations to 3-D [*Várnai*, 1996]. In this case the scaling is $\langle S_k \rangle \sim k^{-3.3}$ for all k. The distribution of β_e is constrained to give a domain average of 30 km^{-1} with 90% of the cloud volume containing cloud droplets.

Figure 10 compares results for a cloud field consisting of cloud top height variations with a constant β_e field (R_{3D} (CVEC)), together with a case which has both cloud top height variations and internal inhomogeneities (R_{3D} (VVEC)). Also shown is a plane-parallel calculation with $\beta_e = 30\ km^{-1}$ (0.5 R_P ($\tau_p = 10$; CVEC)), and a case with a constant cloud top height (flat cloud top) and a variable β_e field (0.5 $R_P(\tau_p = 10$; VVEC)). For the cloud fields with variable cloud top heights (R_{3D}), the increase in reflectance with decreasing μ_o occurs regardless of whether or not internal inhomogeneities are considered. The largest influence of internal inhomogeneities occurs at $\mu_o > 0.5$. Thus Figure 10 shows that while internal inhomogeneities do cause a slight change in the magnitude of reflectances at high solar elevations, they do not have much effect on the relative μ_o dependence. Rather, external inhomogeneities play a far greater role in explaining the observed increase in reflectance with decreasing μ_o given by *Loeb and Davies* [1996].

4. Summary and Conclusions

The purpose of this study was to examine the role of 3-D cloud effects in explaining the results of *Loeb and Davies* [1996]. In that study, observed reflectances averaged over 1 year were shown to increase with solar zenith angle, while 1-D reflectances showed the opposite behavior. Consequently, a systematic bias in 1-D-derived cloud optical depth with solar zenith angle was observed. Based on Monte Carlo simulations involving both stochastic, isotropic, scale-invariant cloud fields and simple cloud geometries, we conclude that 3-D cloud effects associated with cloud sides and cloud top structure are responsible for this discrepancy. When these effects are present, nadir reflectances increase with solar zenith angle in a manner similar to the observations. While this increase is generally most pronounced for vertically extensive broken cloud fields, it can also occur even for overcast clouds with sufficiently inhomogeneous cloud tops (i.e., bumpy tops). This suggests that the solar zenith angle bias in 1-D-derived cloud optical depth retrievals observed for the general cloud scene is likely also present in retrievals from well-defined extensive overcast cloud fields.

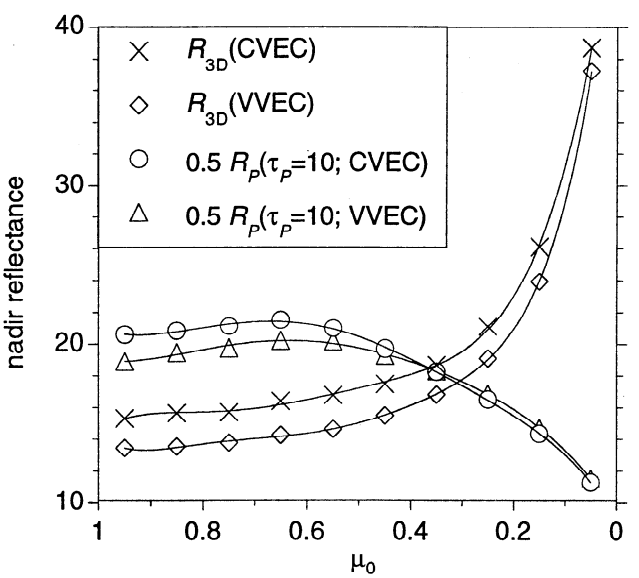

Figure 10. Nadir reflectance versus μ_o for cloud fields with cloud top height variations with a constant volume extinction coefficient (R_{3D} (CVEC)), a variable volume extinction coefficient (R_{3D} (VVEC)), and plane-parallel model calculations with CVEC and VVEC.

The influence of side illumination on nadir reflectance was shown to depend on cloud fraction, cloud aspect ratio, and the distribution of cloud elements within the scene. It is most pronounced for vertically extensive clouds of high aspect ratio. Cloud top structure was also shown to substantially alter the reflected radiation upward at nadir. In calculations involving simple cloud geometries whose surfaces were sloped at different angles relative to the incident solar beam, the increase in nadir reflectance with solar zenith angle was found to be steeper for highly sloped surfaces and occurred at higher solar elevations. These simulations also showed that cloudside illumination and cloud slope contribute nearly equally to the increase in nadir reflectance with solar zenith angle. When reflectances from isolated cones were compared with calculations derived using a simple sloped plane approximation, determined by substituting input incident and observer zenith angles in the 1-D calculations with those relative to a sloped plane and accounting for side illumination, a substantial improvement in the overall nadir reflectance dependence on solar zenith angle was obtained at low solar elevations. The approximation did not remove differences at high Sun caused by diffusive leakage through the cloud sides.

To examine the influence of internal inhomogeneities, associated with small-scale liquid water content variations within clouds, Monte Carlo simulations for cloud fields containing both cloud top height and volume extinction coefficient variations were also considered. Overall, nadir reflectances showed a much smaller sensitivity to internal inhomogeneities than to external inhomogeneities. The largest influence of internal inhomogeneities occurred at high solar elevations, where nadir reflectances were shown to decrease slightly. At low Sun, where the discrepancy between 1-D theory and observations is largest, internal inhomogeneities had a negligible effect.

We conclude from this study, and from the observational study of *Loeb and Davies* [1996], that 3-D effects have an important influence on remote sensing applications involving cloud property retrievals. Clearly, instantaneous errors due to the neglect of 3-D effects for individual cloud scenes do not always simply cancel after averaging over a large number of cases. Further research based on high-resolution narrowband measurements is required in order to quantify 1-D model biases

for both the general scene and for specific scene types (e.g., overcast cloud scenes).

Acknowledgments. This research was supported in part by the Natural Sciences and Engineering Council, the Atmospheric Environment Service (Canada), and the Jet Propulsion Laboratory under contract 959085.

References

Ackerman, B., The nature of meteorological fluctuations in clouds, *J. Appl. Meteorol., 6,* 61–71, 1967.

Barker, H. W., and J. A. Davies, Solar radiative fluxes for stochastic, scale-invariant broken cloud fields, *J. Atmos. Sci., 49,*1115–1126, 1992.

Busygin, V. P., N. A. Yevstratov, and Y. M. Feigel'son, Optical properties of cumulus clouds, and radiant fluxes for cumulus cloud cover, *Izv. Acad. Sci. USSR Atmos. Oceanic Phys.,* Engl. Transl., *9,* 1142–1151, 1973.

Cahalan, R. F., Overview of fractal clouds, in *Advances in Remote Sensing,* pp. 317–389, A. Deepak, Hampton, Va., 1989.

Cahalan, R. F., and J. B. Snider, Marine stratocumulus structure, *Remote Sens. Environ., 28,* 95–107, 1989.

Cannon, J. C., Line transfer in two dimensions, *Astrophys. J., 161,* 255–264, 1970.

Davies, R., The effect of finite geometry on the three-dimensional transfer of solar irradiance in clouds, *J. Atmos. Sci., 35,* 1712–1725, 1978.

Davis, A., P. G. Gabriel, S. Lovejoy, D. Schertzer, and G. L. Austin, Discrete angle radiative transfer, III, Numerical results and applications, *J. Geophys. Res., 95,* 11,729–11,742, 1990.

Harshvardhan, and R. W. L. Thomas, Solar reflection from interacting and shadowing cloud elements, *J. Geophys. Res., 89,* 7179–7185, 1984.

Kobayashi, T., Parameterization of reflectivity for broken cloud fields, *J. Atmos. Sci., 45,* 3034–3045, 1988.

Kobayashi, T., Effects due to cloud geometry on biases in the albedo derived from radiance measurements, *J. Clim., 6,* 120–128, 1993.

Loeb, N. G., and R. Davies, Observational evidence of plane parallel model biases: The apparent dependence of cloud optical depth on solar zenith angle, *J. Geophys. Res., 101,* 1621–1634, 1996.

McKee, T. B., and S. K. Cox, Scattering of visible radiation by finite clouds, *J. Atmos. Sci., 31,* 1885–1892, 1974.

Várnai, T., Reflection of solar radiation by inhomogeneous clouds, Ph.D. thesis, 146 pp., McGill Univ., Montreal, Que., 1996.

Weinman, J. A., and Harshvardhan, Solar reflection from a regular array of horizontally finite clouds, *Appl. Opt., 21,* 2940–2944, 1982.

Welch, R. M., and B. A. Wielicki, Stratocumulus cloud field reflected fluxes: The effect of cloud shape, *J. Atmos. Sci., 41,* 3085–3103, 1984.

Welch, R. M., S. K. Cox, and J. M. Davis, *Solar Radiation and Clouds, Meteorol. Monog.,* vol. *17,* p. 39, Am. Meteorol. Soc., Boston, Mass., 1980.

Wendling, P., Albedo and reflected radiance of horizontally inhomogeneous clouds, *J. Atmos. Sci., 34,* 642–650, 1977.

Wielicki, B. A., and R. M. Welch, Cumulus cloud properties derived using Landsat satellite data, *J. Clim. Appl. Meteorol., 25,* 261–276, 1986.

R. Davies, Department of Atmospheric Sciences and Institute of Atmospheric Physics, The University of Arizona, 1118 E. 4th Street, Rm. 542, P. O. Box 210081, Tucson, AZ 85721-0081. (e-mail: davies@air.atmo.arizona.edu)

N. G. Loeb, College of Oceanic and Atmospheric Sciences, Oregon State University, Corvallis, OR 97331. (e-mail: norman@light.ats.orst.edu)

T. Várnai, Department of Atmospheric and Oceanic Sciences, McGill University, 805 Sherbrooke St., Montreal, Quebec, Canada H3A 2K6. (e-mail: tamas@zephyr.meteo.mcgill.ca)

(Received August 16, 1996; revised November 8, 1996; accepted November 11, 1996.)